Available online at www.sciencedirect.com
ScienceDirect
Journal of Sound and Vibration 323 (2009) 530–554
JOURNAL OF SOUND AND VIBRATION
www.elsevier.com/locate/jsvi

Optimal resonant control of flexible structures

Steen Krenk*, Jan Høgsberg

Department of Mechanical Engineering, Technical University of Denmark, DK-2800 Lyngby, Denmark

Received 16 October 2008; received in revised form 9 January 2009; accepted 13 January 2009
Handling Editor: C.L. Morfey
Available online 23 February 2009

Abstract

When introducing a resonant controller for a particular vibration mode in a structure this mode splits into two. A design principle is developed for resonant control based on equal damping of these two modes. First the design principle is developed for control of a system with a single degree of freedom, and then it is extended to multi-mode structures. A root locus analysis of the controlled single-mode structure identifies the equal modal damping property as a condition on the linear and cubic terms of the characteristic equation. Particular solutions for filtered displacement feedback and filtered acceleration feedback are developed by combining the root locus analysis with optimal properties of the displacement amplification frequency curve. The results are then extended to multi-mode structures by including a quasi-static representation of the background modes in the equations for the damped mode. Applications to multi-degree-of-freedom systems are illustrated by idealized models of a piezoelectric sensor–actuator device on a beam and an accelerometer–actuator device on a cable. In both cases near-ideal response characteristics are obtained, when including the quasi-static correction of the modal properties.
© 2009 Elsevier Ltd. All rights reserved.

1. Introduction

An important aspect of the use of control of structures is to limit the dynamic response around the natural resonances of the structure. A particular instance is the use of a resonant damped mass in the form of a tuned mass absorber. The underlying theory has remained virtually unchanged since the work of Den Hartog in the thirties [1]. The classic tuned mass absorber design procedure is based on analysis of the frequency response curve for a harmonically forced oscillator. This procedure is rather different from the methods typically used in the design of control systems, where some form of root locus analysis often forms a central ingredient, and the control force is mostly represented via a proportional gain factor. This paper presents a combined design method for resonant control, in which a root locus analysis is used to identify the optimal frequency of the resonant controller by imposing a requirement of equal damping of the two modes generated by the interference of the controller with the structural mode to be controlled. The feedback, coupling the resonator to the structure, is designed subsequently by using properties of the frequency response curve of the controlled modal response. Thus, the present method combines the root locus approach of control theory with the

*Corresponding author. Tel.: +45 45 25 19 64.
E-mail address: sk@mek.dtu.dk (S. Krenk).

0022-460X/$ - see front matter © 2009 Elsevier Ltd. All rights reserved.
doi:10.1016/j.jsv.2009.01.031

frequency response characteristics typical of structural analysis. This section presents an overview of some central contributions to the control theory approach to resonant control, as well as key references to the structural vibration approach.

Damping of flexible structures by collocated active control dates back to the late seventies in connection with damping of large space structures. The basic strategy with direct velocity feedback control was proposed by Balas [2], representing an active implementation of a pure dissipative viscous damper model. In principle this simple control strategy may perform satisfactorily for many engineering problems, but it was demonstrated by Goh and Caughey [3] that the inclusion of the actuator dynamics may lead to stability problems. It is therefore often desirable to filter the sensor input by second-order filter as introduced for positive position feedback by Fanson and Caughey [4] and for acceleration feedback by Sim and Lee [5]. For control strategies with second-order filters additional efficiency can be obtained by making use of the inherent resonant characteristics, as observed for acceleration feedback by Juang and Phan [6]. The implementation of a resonant control filter introduces an additional resonance represented by a new pole in the complex plane, and common design techniques are mostly based on some form of pole placement, Goh and Yan [7], where maximum damping is achieved at the bifurcation point of the structural and controller mode, see e.g. de Noyer and Hanagud [8]. Alternative design procedures determine the filter parameters for instance by minimizing a quadratic cost function in the structural response variables [9,10] or by maximizing the energy dissipation in the actuator [11]. The range of applications of resonant controllers is fairly large, covering e.g. damping of slender beams by piezoelectric sensor/actuator systems [12,13] and mitigation of earthquake induced vibrations of shear frame structures [14].

A common characteristic of most of the work on resonant control from a control theory perspective is its focus of the location of the poles in the complex plane. However, optimal response characteristics also require optimal coupling between control and structure, and may also involve the load-properties that do not show up directly in the root locus diagram.

The traditional approach to resonant control within the structural dynamics community has been more or less opposite that within control theory, with the full analysis and calibration relying on observable characteristics of the frequency response curve. The original design procedure for the tuned mass absorber by Ormondroyd and Den Hartog [1,15] has remained virtually unchanged to this day. The analysis is separated into two parts. First the optimum absorber frequency is determined by considering two points on the frequency response curve, that are independent of the imposed damping. The damping is selected subsequently to form a flat plateau on the frequency response curve, typically by the procedure proposed by Brock [16]. A recent analysis by Krenk [17] has demonstrated that equal amplification at the fix points of the frequency response curve corresponds to equal damping of the two modes generated by the interference between the structure and the additional mass. It was also demonstrated that improved damping could be obtained by changing the design criterion to one imposing equal amplification at three selected points on the frequency response curve.

An important aspect of a theoretical design procedure, initially developed for a single degree of freedom structure, is the extension to structures with many degrees of freedom. In the case of tuned mass dampers a simple iterative procedure may be sufficient for stiff structures that retain their vibration modes fairly intact after installing the mass absorber(s), [18]. However, it is generally desirable, and necessary for very flexible structures, to account for the effect of that part of the full structural response, that is not directly associated with the mode to be controlled. This problem has been addressed in connection with a tuned mass absorber on a multi-degree-of-freedom structure by Ozer and Royston [19,20], who included the additional degree of freedom by use of the Sherman–Morrison formula and established an analogy with the single degree of freedom system and the design procedure of Den Hartog. In its general form the procedure is rather cumbersome, involving an iteration process.

This paper presents a design method for resonant control systems consisting of a resonant second-order filter, connected to a structure by displacement or acceleration feedback, that is passed through a simple filter, that enables the introduction of an appropriate moderate phase shift. The basic features are close to, and include, those of the tuned mass absorber. The general features of the problem are as follows. The resonant device is tuned to a frequency close to the natural frequency of the structure—either a single-degree of freedom system or a selected modal frequency of a multi-degree of freedom system. The coupling leads to a split of the

original structural mode into two modes with closely spaced frequencies. For small damping these frequencies show up in the frequency response curve of the structural response as two closely spaced peaks. The design problem consists in the selection of the parameters to make the device resonant and introduce an amount of damping that makes the combined structural response exhibit a frequency interval around the natural frequencies of the two coupled modes with large uniform damping. The dependence of these features on the device parameters is highly nonlinear, and optimal calibration must be considered in a qualitative sense due to the local character of the problem.

The design for control of an ideal single-degree-of-freedom structure proceeds in two steps. First a root locus analysis identifies the oscillator frequency to produce equal modal damping. The general properties of the root locus diagram corresponding to equal modal split of the damping ratio is presented in Section 3. Section 4 presents the two basic cases of resonant control by displacement and acceleration feedback, respectively. First the resonance frequency is determined from the root locus analysis, and then the actuator feedback filter parameters are determined from a frequency analysis. Finally, the design procedure is extended to multi-degree-of-freedom-structures in Section 5 by accounting for the non-damped background modes via a quasi-static approximation. The result is a modified set of explicit formulae for the control parameters. It is demonstrated by examples that this extends the quality of the single-degree-of freedom results to flexible structures, retaining the nearly equal modal damping characteristic and enabling a considerable increase of imposed damping relative to typical passive damping devices.

2. Generic frequency response format

The analysis and design of the system will be carried out in the frequency domain. For this purpose the time dependence is represented via the complex exponential function $\exp(i\omega t)$, where ω is the angular frequency, that will typically be complex valued, corresponding to attenuated response.

The controller force F_c is obtained from a control variable y, which in turn is obtained by filtering the response x. This can be expressed in the general frequency format

$$G_{xx}(\omega)x + G_{xy}(\omega)y = F/m$$

$$G_{yx}(\omega)x + G_{yy}(\omega)y = 0 \tag{1}$$

where F is the external force, and m is the structural mass. $G_{xx}, G_{xy}, \ldots$ are frequency dependent transfer functions. For a structure without internal damping the natural angular frequency ω_s is given in terms of the stiffness k and mass m as

$$\omega_s^2 = k/m \tag{2}$$

Thus, the free response of the structure is governed by the frequency function

$$G_{xx}(\omega) = \omega_s^2 - \omega^2 \tag{3}$$

In this formulation the effect of structural damping has been omitted. Numerous investigations have demonstrated that even for the special case of a 'tuned mass absorber' the introduction of structural damping in the equations used to develop optimal design criteria prevents the development of tractable analytical solutions. The usual procedure is therefore to base the development of the design formulas on an undamped structural system, and then to introduce the damping device calibrated in this way into the damped structural model. The effect of the structural damping is included by appeal to approximate formulas giving the combined modal damping in terms of the structural modal damping and that obtained from the resonant damping device. As demonstrated in [21] the modal structural damping ratio ζ_s is included additively in the resulting modes with the resonant device by 50–75%, depending on the relative magnitude of structural to resonant damping. Thus, a conservative and rather representative contribution of the structural damping is obtained by estimating a contribution of 50% of the original modal structural damping. For steel structures where additional resonant damping is needed the original damping ratio is typically of the order $\zeta_s \simeq 0.2-0.4\%$, while the desired damping is about 10 times larger. Thus, the contribution from the original structural damping is negligible in these cases.

The controller consists of an oscillator defined by the second-order filter function

$$G_{yy}(\omega) = \omega_c^2 - \omega^2 + 2\mathrm{i}\zeta_c\omega_c\omega \tag{4}$$

where ω_c represents a characteristic angular frequency, and the non-dimensional parameter ζ_c defines the bandwidth of the filter. In the case of a tuned mass vibration absorber ω_c and ζ_c are simply the undamped natural frequency and the damping ratio of the suspended mass system if connected to a rigid support [1,17]. The function $G_{yx}(\omega)$ defines the output from the structure to be used by the controller, and $G_{xy}(\omega)$ defines the frequency dependence of the feedback force on the structure. The quality of the device depends on the characteristics of the four frequency functions $G_{xx},\ldots,G_{xy}$. Before discussing the specific form of the feedback functions G_{xy} and G_{yx}, defining the coupling of the system, some general properties of optimal damping by resonant control by a system of the form defined by relations (1) will be studied in the next section.

The quality of the control is associated with its ability to limit the response of the structure around the resonance frequency ω_s. The response x follows from elimination of the control variable y between Eq. (1), whereby

$$x = \frac{G_{yy}}{G_{xx}G_{yy} - G_{xy}G_{yx}}\frac{F}{m} \tag{5}$$

Clearly, the magnitude of the control force F_c needed to reduce the resonant response is also of importance. It follows from (1) in the form

$$F_c = -mG_{xy}y = \frac{G_{xy}G_{yx}}{G_{xx}G_{yy} - G_{xy}G_{yx}}F \tag{6}$$

It is seen that interchange of G_{xy} with G_{yx} may lead to a redefinition of the control variable y, but leaves the structural response x unchanged.

3. Root locus diagram

For systems in which the frequency functions $G_{xx},\ldots,G_{yy}$ are quadratic polynomials, corresponding to second-order filters, the resulting characteristic polynomial appearing as denominator in expressions (5) and (6) for the structural response and the control force, respectively, is a quartic polynomial. It follows from the representation of the response in terms of the complex exponential $\mathrm{e}^{\mathrm{i}\omega t}$ that the coefficients of the even order terms are real, while the coefficients of the odd order terms contain the imaginary unit i. In Ref. [17] it was demonstrated for the special case corresponding to a tuned mass absorber that equal modal damping would result from a suitable calibration of the natural frequency of the tuned mass. Here the argument is turned around, and the generic format of the characteristic equation is constructed from the requirement that the coupled system should have modes with equal damping ratio. In this section the root locus analysis of the denominator is carried out with generic parameters, and specific filter variables are introduced in connection with the response analysis in Section 4.

Let the four roots of the characteristic equation be denoted $\omega_1,\ldots,\omega_4$, and assume that there is a parameter combination for which ω_1 and ω_2 lie in the first quadrant. The corresponding modes will then have equal damping ratio, if ω_1 and ω_2 lie on the same line containing the origin of the complex plane. This implies that they are inverse points in the complex plane with respect to a circle with radius equal to some real-valued frequency ω_0, i.e.

$$\frac{\omega_2}{\omega_0} = \frac{\omega_0}{\omega_1^*} \tag{7}$$

where ω_1^* denotes the conjugate of ω_1. This relation is illustrated in Fig. 1. The reciprocal relation between ω/ω_0 and ω_0/ω suggests the following format of the characteristic equation:

$$\left(\frac{\omega}{\omega_0} - \frac{\omega_0}{\omega}\right)^2 - 4\mathrm{i}\beta c\left(\frac{\omega}{\omega_0} - \frac{\omega_0}{\omega}\right) - 4c^2 = 0 \tag{8}$$

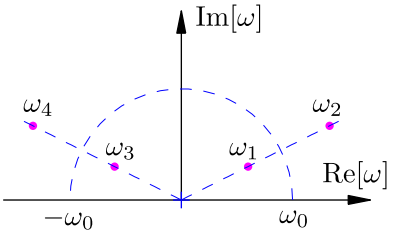

Fig. 1. Complex roots ω_1, ω_2 and ω_3, ω_4 as inverse points of circle $|\omega| = \omega_0$.

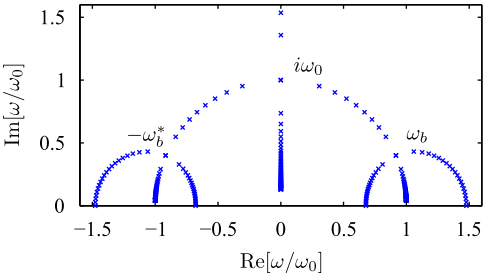

Fig. 2. Root locus diagram for $c = 0.4$.

This equation contains two coefficients, and it turns out to be convenient to express these in terms of the real-valued parameters c and β as shown. By taking the complex conjugate to this equation it follows that if ω_1 is a root, so is ω_2 as defined by Eq. (7). Furthermore, the two remaining roots are given by $\omega_{3,4} = -\omega_{1,2}^*$ as illustrated in Fig. 1. This property is required by the origin of the equation from real-valued filters in the time domain. Thus, it has been demonstrated that the format (8) does indeed define the characteristic equation of a resonant system with equal modal damping. The corresponding polynomial form follows from multiplication with $(\omega_0\omega)^2$:

$$\omega^4 - (2 + 4c^2)\omega_0^2\omega^2 + \omega_0^4 - 4\mathrm{i}\beta c\omega_0\omega(\omega^2 - \omega_0^2) = 0 \tag{9}$$

It is seen that the reference frequency ω_0 is defined by the constant term of the normalized characteristic polynomial. The special property of equally damped modes as expressed by the inverse root relation (7) is equivalent to imposing a balance constraint between the cubic and linear terms of the equation. This constraint implies that the cubic and linear terms cancel for $\omega = \pm\omega_0$.

A full analysis of the root locus diagram is presented in Appendix A. The general form is illustrated in Fig. 2 for a fixed value of the parameter $c = 0.4$. The markers correspond to $\beta = 0, 0.05, 0.10, 0.15, \ldots$. For $\beta = 0$ the four roots ω_1, ω_2 and ω_3, ω_4 are located symmetrically on the real axis with distance $\omega_2 - \omega_1 = \omega_3 - \omega_4 = 2c\omega_0$. When the parameter β is increased from zero, the roots ω_1, ω_2 and ω_3, ω_4 generate branches that meet at two bifurcation points for $\beta = 1$, corresponding to

$$\omega_b/\omega_0 = \mathrm{i}c \pm \sqrt{1 - c^2} \tag{10}$$

When β is increased beyond 1 the roots follow the circle $|\omega| = \omega_0$, centered at the origin with radius ω_0. Two of these branches converge towards the points $\pm\omega_0$ on the real axis, while the two other branches meet at a new bifurcation point at $\mathrm{i}\omega_0$, where they branch along the imaginary axis. The relevant parametrization is given in Appendix A.

The root locus branches of main interest in the present context are those traced by the parameter interval $0 \leqslant \beta \leqslant 1$. On these parts all four roots correspond to the same damping ratio, and the magnitude of this damping ratio is a main objective of the design of the system. It is therefore of considerable interest to obtain an expression for this damping ratio in terms of the system parameters c and β. To this purpose the characteristic equation (9) is written in terms of the roots $\omega_1, \ldots, \omega_4$ in the form

$$(\omega - \omega_1)(\omega - \omega_2)(\omega - \omega_3)(\omega - \omega_4) = 0 \tag{11}$$

Comparison of the coefficient of the cubic term of this equation with the corresponding coefficient of Eq. (9) yields the relation

$$4\mathrm{i}\beta c = (\omega_1+\omega_2+\omega_3+\omega_4)/\omega_0 = 2\mathrm{i}\,\mathrm{Im}\left[\frac{\omega_1}{\omega_0}-\frac{\omega_0}{\omega_1}\right] \tag{12}$$

where the reflection properties shown in Fig. 1 have been used. The damping ratio ζ of the combined system is defined by the normalized imaginary part of the characteristic frequencies,

$$\omega_1 = |\omega_1|(\sqrt{1-\zeta^2}+\mathrm{i}\zeta) \tag{13}$$

Substitution of this representation into Eq. (12) leads to the following expression for the damping ratio:

$$\zeta = \frac{\beta c}{\frac{1}{2}\left(\frac{|\omega_1|}{\omega_0}+\frac{\omega_0}{|\omega_1|}\right)} \simeq \beta c \tag{14}$$

The last expression is based on the approximation that the denominator is unity. In fact it follows from Eq. (A.4) that the value of the denominator decreases from $\sqrt{1+c^2}$ for $\beta=0$ to unity at the bifurcation point for $\beta=1$. Thus, the error of this approximation is small for small values of c, typical of applications.

The parameters c and β can now be given direct physical interpretations. The bifurcation points ω_b on the smaller contours correspond to $\beta=1$, and it then follows from Eq. (14) that

$$c \simeq \zeta_b \tag{15}$$

The parameter β then follows by elimination of c from Eq. (14),

$$\beta \simeq \zeta/\zeta_b \tag{16}$$

i.e. as the actual damping ratio relative to the bifurcation value ζ_b.

The root locus diagram in Fig. 2 shows the root locations as function of the parameter β for a fixed value of c. In an actual design context it is more pertinent to consider the roots as located at optimal positions on the smaller contours by a specific value of the parameter β. Increasing damping is then obtained by increasing the parameter c. As demonstrated later optimal response characteristics are obtained by selecting $\beta \simeq \sqrt{2}/2$. This value represents a optimal compromise between the introduction of sufficient damping and a sufficient separation of the natural frequencies ω_1 and ω_2 to avoid direct superposition of the modes. The asymptotic behavior of the roots ω_1 and ω_2 then follows from combination of relations (A.2) and (A.3), whereby

$$\omega_{1,2}/\omega_0 \simeq 1+\tfrac{1}{2}\sqrt{2}(\mp 1+\mathrm{i})c \tag{17}$$

This relation indicates that the normalized roots move from ω_0 into the upper half-plane under an initial angle of 45° with the real axis. This is illustrated in Fig. 3, showing the root locus diagram for $\beta=\sqrt{2}/2$ and $c=0,0.1,0.2,\ldots$.

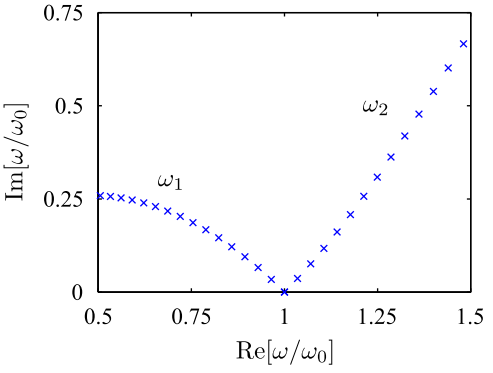

Fig. 3. Root locus diagram for $\beta=\sqrt{2}/2$.

4. Frequency response analysis

The root locus analysis of the previous section has identified a characteristic angular frequency ω_0 and determined a condition for equal modal damping in terms of ω_0. The equal modal damping condition is determined by a combination of all four frequency functions $G_{xx},\ldots,G_{yy}$. The remaining conditions are determined from the frequency response (5) of the structural response x and the frequency response (6) of the control force F_c. It is desirable that the control force vanishes at zero frequency as well as at infinite frequency. The product $G_{xy}G_{yx}$, appearing as numerator of the control force, must therefore be a polynomial containing only linear, quadratic and cubic terms. In this section the two special cases corresponding to displacement feedback and acceleration feedback are treated in detail. Each of these cases are defined by two terms, providing the real part and an appropriate phase shift via the imaginary part.

4.1. Filtered displacement feedback

In this case the feedback is based on the displacement, leading to a constant frequency function

$$G_{yx}(\omega)=\omega_c^2 \tag{18}$$

The frequency ω_c from the resonant controller has been used for dimensional reasons. The actuator frequency function G_{xy} combines a quadratic and a linear term in ω in order to enable tuning of the phase,

$$G_{xy}(\omega)=\alpha\omega^2+\gamma 2\mathrm{i}\zeta_c\omega_s\omega \tag{19}$$

Here the structure reference frequency ω_s has been used, and two non-dimensional gain factors α and γ have been introduced. The design problem consists of the determination of optimal combinations of the frequency ratio ω_c/ω_s, the bandwidth parameter ζ_c, and one of the two gain parameters α and γ. The remaining gain parameter serves as the gain of the optimized system. The procedure consists in first introducing equal modal damping properties, and then optimizing the frequency response curve.

As demonstrated in Section 3 equal modal damping is achieved by imposing an appropriate balance between the linear and cubic term in the denominator of the response expressions (5) and (6),

$$G_{xx}G_{yy}-G_{xy}G_{yx}=\omega^4-[\omega_s^2+(1+\alpha)\omega_c^2]\omega^2+\omega_s^2\omega_c^2-2\mathrm{i}\zeta_c\omega_c\omega[\omega^2-\omega_s^2+\gamma\omega_s\omega_c] \tag{20}$$

The reference frequency ω_0 of this equation follows from the constant term, whereby

$$\omega_0^2=\omega_s\omega_c \tag{21}$$

Thus, the reference frequency ω_0 is the geometric mean value of the original structure frequency ω_s and the controller frequency ω_c. Equal modal damping is obtained by setting the constant term in the square brackets of the last term equal to ω_0^2:

$$\omega_s^2-\gamma\omega_s\omega_c=\omega_0^2 \tag{22}$$

Upon substitution of ω_0 from Eq. (21) it follows that

$$\omega_c=\frac{\omega_s}{1+\gamma} \tag{23}$$

Finally, an explicit expression for the reference frequency ω_0 follows by substitution of this expression for ω_c into Eq. (21),

$$\omega_0^2=\frac{\omega_s^2}{1+\gamma} \tag{24}$$

Thus, the equal modal damping condition has determined the controller resonance frequency ω_c and defined the reference frequency ω_0 in terms of the gain parameter γ.

The optimal values of the damping parameter ζ_c and the gain parameter α are determined from the frequency response curve. The principle is illustrated in Fig. 4. Within the present filter format the displacement amplification curve is independent of the damping parameter ζ_c at two points—the so-called fix

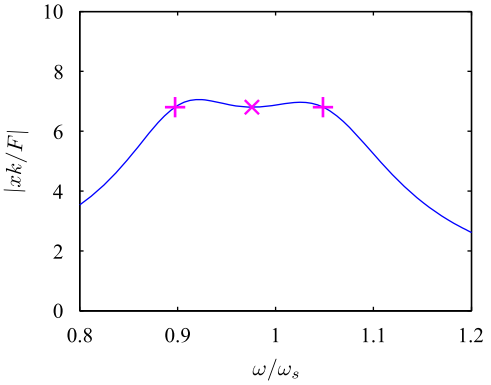

Fig. 4. Equal displacement amplification at three frequencies.

points—occurring at frequencies ω_A and ω_B. The requirement of equal amplification at ω_A and ω_B provides an equation for the parameter α. It turns out that the reference frequency ω_0 lies within the interval between the two fix points, i.e. $\omega_A<\omega_0<\omega_B$. Flat response characteristics are therefore imposed by setting the amplification at ω_0 equal to the amplification at the fix points ω_A and ω_B. The result of these two conditions is illustrated in Fig. 4. These two conditions have been used in connection with the tuned mass absorber, where the equal amplification at fix points was introduced in Ref. [1] and the equal amplification at the intermediate frequency in Ref. [17]. The analysis is straightforward, but somewhat lengthy, and is therefore given in Appendix B.

As shown in the Appendix equal displacement amplification at the fix points ω_A and ω_B determines the gain parameter α as

$$\alpha = \gamma(1-\gamma) \tag{25}$$

The equal amplification condition at the reference frequency ω_0 then gives the optimal damping ratio by

$$\zeta_c^2 = \frac{\gamma}{4}\frac{2+\gamma}{1+\gamma} \tag{26}$$

Thus, the control system parameters ω_c, ζ_c and α have all been expressed in terms of the gain parameter γ.

The present parameter calibration has the interesting property that each of the equally damped modes have approximately half of the damping ratio ζ_c introduced in the controller. This follows from the generic result (12), when applied to the present calibrated filter combination. The product β_c in the generic equation is expressed in terms of the current specific parameters by comparison of the cubic terms in the generic frequency equation (9) and the present frequency equation (20). As a result the modal damping ratio is expressed as

$$\zeta \simeq \frac{1}{2}\zeta_c\frac{\omega_c}{\omega_0} \simeq \frac{1}{2}\zeta_c \tag{27}$$

This approximate result is very accurate for realistic damping ratio values. It serves as a convenient starting point in designing an appropriate resonant filter, when a desired modal damping ratio ζ is known, as illustrated in Section 5. The equal split of the imposed damping to the modes was observed in the case of a tuned mass damper in Ref. [17] and used in designing a tuned damping system for a pedestrian bridge in Ref. [18].

For the case of displacement feedback the final form of the displacement response in terms of the optimal parameters follows from Eq. (5) as

$$\frac{xk}{F} = \frac{(1+\gamma)\omega_0^2[\omega_0^2-(1+\gamma)\omega^2+\mathrm{i}\sqrt{\gamma(2+\gamma)}\omega_0\omega]}{(1+\gamma)\omega^4-(2+3\gamma)\omega_0^2\omega^2+(1+\gamma)\omega_0^4+\mathrm{i}\sqrt{\gamma(2+\gamma)}\omega_0\omega(\omega_0^2-\omega^2)} \tag{28}$$

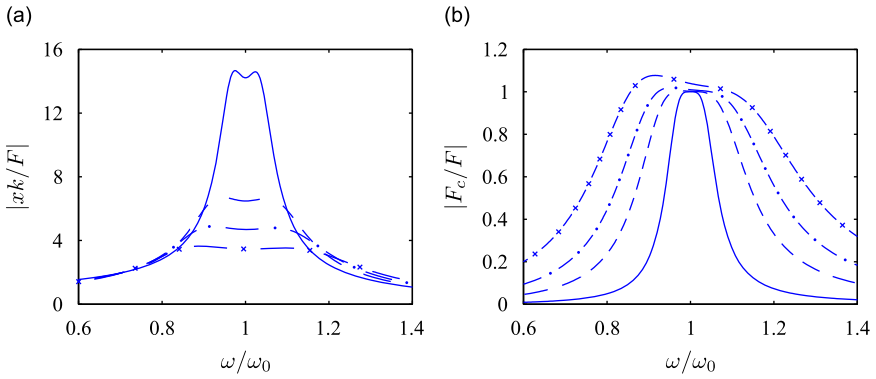

Fig. 5. Filtered displacement feedback, $\gamma = 0.01$ (——), 0.05 (– – –), 0.1 (– · –) and 0.2 (– × –). (a) Displacement amplitude. (b) Control force amplitude.

The relative magnitude of the control force follows from Eq. (6). For optimal parameters the result is

$$\frac{F_c}{F} = \frac{\gamma\omega_0^2[(1-\gamma)\omega^2 + \mathrm{i}\sqrt{\gamma(2+\gamma)}\omega_0\omega]}{(1+\gamma)\omega^4 - (2+3\gamma)\omega_0^2\omega^2 + (1+\gamma)\omega_0^4 + \mathrm{i}\sqrt{\gamma(2+\gamma)}\omega_0\omega(\omega_0^2-\omega^2)} \tag{29}$$

The displacement and control force amplitudes are shown in Fig. 5. Both sets of curves display a plateau-like behavior around the structural frequency ω_s. The displacement amplification at the fix points and the reference frequency ω_0 is given by Eq. (B.11) as

$$\left|\frac{xk}{F}\right|_{\omega_0} = (1+\gamma)\sqrt{\frac{2(1+\gamma)}{\gamma}} \simeq \sqrt{2/\gamma} \tag{30}$$

where the last expression is the asymptotic value for small gain γ. The control force around the resonance frequency is approximately equal to the external force and given by

$$\left|\frac{F_c}{F}\right|_{\omega_0} = \sqrt{1+2\gamma^2} \simeq 1+\gamma^2\cdots \tag{31}$$

Thus, in the case of displacement feedback the control force at the reference frequency ω_0 increases with the gain parameter γ. However, as seen from the graphs in Fig. 5 this increase is negligible for $\gamma \lesssim 0.1$, corresponding to the amplification factor $\sqrt{2/0.1} \simeq 4.5$, which in practice is a very large damping of the resonance. Thus, for practical levels of damping the skewness of the control force curve and the change of peak value will be negligible.

4.2. Filtered acceleration feedback

This section describes the equal modal damping design of a system with acceleration feedback, e.g. from an accelerometer. This corresponds to the controller being driven via the frequency function

$$G_{yx}(\omega) = \omega^2 \tag{32}$$

In order for the control force to attenuate for increasing large frequencies the product $G_{xy}G_{yx}$ must be limited to a cubic polynomial. That leads to the following two-parameter format:

$$G_{xy}(\omega) = \alpha\omega_c^2 + \gamma 2\mathrm{i}\zeta_c\omega_c\omega \tag{33}$$

with gain factors α and γ. The design problem consists in the determination of optimal combinations of the frequency ratio ω_c/ω_s, the bandwidth parameter ζ_c, and the two gain parameters α and γ. The procedure is similar to that of the displacement feedback problem treated above.

In the present case of acceleration feedback the denominator of the response and control force takes the form

$$G_{xx}G_{yy} - G_{xy}G_{yx} = \omega^4 - [\omega_s^2 + (1+\alpha)\omega_c^2]\omega^2 + \omega_s^2\omega_c^2 - 2\mathrm{i}\zeta_c\omega_c\omega[(1+\gamma)\omega^2 - \omega_s^2] \tag{34}$$

The reference frequency ω_0 of this equation follows from the constant term as

$$\omega_0^2 = \omega_s\omega_c \tag{35}$$

It is observed that this is the same as in the case of displacement feedback, because the product $G_{xy}G_{yx}$ does not contain a constant term. As discussed previously this is a necessary condition for the control force to vanish at zero frequency. The equal modal damping property follows from normalization of the two terms in the square brackets of the last term:

$$\omega_0^2 = \frac{\omega_s^2}{1+\gamma} \tag{36}$$

Combination of these two relations gives

$$\omega_c = \frac{\omega_0}{\sqrt{1+\gamma}} = \frac{\omega_s}{1+\gamma} \tag{37}$$

The expressions for the control frequency ω_c and the reference frequency ω_0 are identical to those obtained for the case of displacement feedback.

As shown in Appendix B equal amplification at the fix point frequencies ω_A and ω_B leads to the gain parameter

$$\alpha = \gamma \tag{38}$$

The equal amplification condition at the reference frequency ω_0 then gives

$$\zeta_c^2 = \frac{1}{2}\frac{\gamma}{1+\gamma} \tag{39}$$

It is seen that the expressions for α and ζ_c obtained here for acceleration feedback are different from those corresponding to displacement feedback. However, they exhibit the same asymptotic dependence on γ for small values of this parameter. The equal split of the imposed damping ratio ζ_c to the two modes as expressed in Eq. (27) is also valid in the case of acceleration feedback.

For the case of acceleration feedback the final form of the displacement response in terms of the optimal parameters follows from Eq. (5) as

$$\frac{xk}{F} = \frac{\omega_0^2[\omega_0^2 - (1+\gamma)\omega^2 + \mathrm{i}\sqrt{2\gamma}\omega_0\omega]}{\omega^4 - (2+\gamma)\omega_0^2\omega^2 + \omega_0^4 + \mathrm{i}\sqrt{2\gamma}\omega_0\omega(\omega_0^2 - \omega^2)} \tag{40}$$

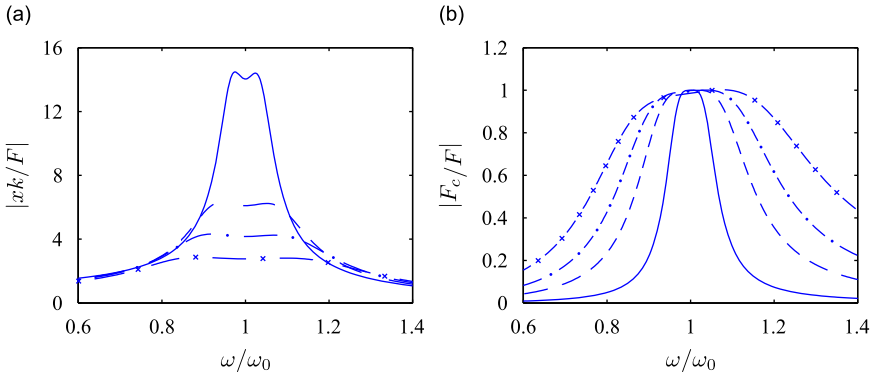

Fig. 6. Filtered acceleration feedback, $\gamma = 0.01$ (——), 0.05 (– – –), 0.1 (– · –) and 0.2 (– × –). (a) Displacement amplitude. (b) Control force amplitude.

The relative magnitude of the control force follows from Eq. (6). For optimal parameters the result is

$$\frac{F_c}{F}=\frac{\gamma}{1+\gamma}\frac{\omega_0^2\omega^2+\mathrm{i}\sqrt{2\gamma}\omega_0\omega^3}{\omega^4-(2+\gamma)\omega_0^2\omega^2+\omega_0^4+\mathrm{i}\sqrt{2\gamma}\omega_0\omega(\omega_0^2-\omega^2)} \tag{41}$$

The frequency response for the structure displacement x and the control force F_c are illustrated in Fig. 6. It is seen that the displacement amplitude has a fairly level plateau with amplitude given by Eq. (B.20) as

$$\left|\frac{xk}{F}\right|_{\omega_0}=\sqrt{\frac{2+\gamma}{\gamma}}\simeq\sqrt{2/\gamma} \tag{42}$$

The control force has a plateau-like behavior with a slight upward slope towards increasing frequencies. In addition, there is a slight dependence on the gain parameter of the form

$$\left|\frac{F_c}{F}\right|_{\omega_0}=\frac{\sqrt{1+2\gamma}}{1+\gamma}\simeq 1-\frac{1}{2}\gamma^2\cdots \tag{43}$$

It is seen that the frequency curves in this case have a small upward inclination with increasing frequency, but again the effect is small for gain values likely to be used in practice.

5. Multi-degree-of-freedom systems

Results for single degree for freedom systems can often be calibrated so that they are representative for modal behavior in multi-degree-of-freedom systems. The typical problem is that the individual mode only accounts for part of the motion registered by a control sensor, and similarly the actuator force excites other modes as well. This is the so-called 'spillover' problem. The basic form, in which a truncated modal analysis is supplemented by a quasi-static representation of the remaining modes goes back to the seventies [22], while the introduction of a quasi-static term in truncated modal analysis has been discussed e.g. in Ref. [13]. In this section the idea of a quasi-static correction term is used to account for the fact that a displacement or acceleration sensor on a multi-degree-of-freedom structure also registers the motion from non-resonant background modes. This effect should be included when establishing the analogy with resonant control of a single-degree-of-freedom system, analyzed in the previous sections. The present discussion starts with establishing an equivalent two-component set of equations for the resonant control including an approximate representation of the effect of background modes, and then proceeds to illustrate the detailed procedure for displacement feedback and acceleration feedback, respectively.

5.1. Correction for background modes in MDOF systems

Consider a multi-degree-of-freedom system with stiffness matrix $\mathbf{K}$ and mass matrix $\mathbf{M}$. The displacements are denoted $\mathbf{q}$ and the corresponding external loads $\mathbf{F}$. In addition to the external load an actuator with control signal η is connected to the structure as described by the connectivity vector $\mathbf{w}$. The connectivity vector $\mathbf{w}$ contains the number 1 at the appropriate degree-of-freedom if it is connected to the surroundings, and a set of numbers 1 and -1 for degrees-of-freedom that are connected by an actuator. The corresponding frequency equation is

$$(\mathbf{K}-\omega^2\mathbf{M})\mathbf{q}=\mathbf{F}-\mathbf{w}G_{q\eta}(\omega)\eta \tag{44}$$

The actuator is assumed to be controlled by a collocated signal, i.e. a signal generated by a sensor attached to the same degrees-of-freedom as the actuator. Thus, the actuator signal η is controlled by the frequency equation

$$G_{\eta\eta}(\omega)\eta=-G_{\eta q}(\omega)\mathbf{w}^{\mathrm{T}}\mathbf{q} \tag{45}$$

A modal representation of the response is introduced in the form

$$\mathbf{q}=\sum\nolimits_j\mathbf{u}_j x_j,\quad \mathbf{u}_j^{\mathrm{T}}\mathbf{M}\mathbf{u}_k=\delta_{jk} \tag{46}$$

where $\mathbf{u}_j$ denotes the jth mode shape vector, and x_j the corresponding modal amplitude. δ_{jk} denotes Kronecker's delta, whereby the modes are normalized to unity with respect to the mass matrix.

Here the case of a single collocated controller is developed, and to be specific the controller is assumed to aim at controlling the first mode. The corresponding modal equation is obtained from Eq. (44) by pre-multiplication with the modal vector $\mathbf{u}_1^{\mathrm{T}}$. This gives an equation of the form

$$G_{qq}(\omega)x_1 + v_1 G_{q\eta}(\omega)\eta = 0 \tag{47}$$

with the modal frequency response function in terms of the undamped modal frequency ω_1,

$$G_{qq}(\omega) = \omega_1^2 - \omega^2 \tag{48}$$

The coefficient v_1 describes the (relative) motion of the actuator for the normalized mode $\mathbf{u}_1$,

$$v_1 = \mathbf{u}_1^{\mathrm{T}}\mathbf{w} \tag{49}$$

It is therefore to be expected that this factor appears on the actuator term in Eq. (47).

While the actuator force is included directly in the modal equation (44) by projection on the mode shape vector $\mathbf{u}_1$, the term $\mathbf{w}^{\mathrm{T}}\mathbf{q}$ from the displacement vector in the control equation (45) contains contributions from all modes. For flexible structures it is important to include the effect of these 'background modes' in the calibration of the control parameters. The purpose is to identify the optimal parameters, and the displacement vector $\mathbf{q}$ is therefore eliminated by use of the homogeneous form of Eq. (44),

$$\mathbf{w}^{\mathrm{T}}\mathbf{q} = -\mathbf{w}^{\mathrm{T}}(\mathbf{K} - \omega^2\mathbf{M})^{-1}\mathbf{w}G_{q\eta}(\omega)\eta \tag{50}$$

The inverse of the dynamic stiffness matrix can be expanded in terms of the mode shape vectors as

$$(\mathbf{K} - \omega^2\mathbf{M})^{-1} = \sum_j \frac{\mathbf{u}_j\mathbf{u}_j^{\mathrm{T}}}{\omega_j^2 - \omega^2} \tag{51}$$

The corresponding static result is obtained for $\omega = 0$,

$$\mathbf{K}^{-1} = \sum_j \frac{\mathbf{u}_j\mathbf{u}_j^{\mathrm{T}}}{\omega_j^2} \tag{52}$$

A quasi-static approximation is obtained by including only the full form from the resonant mode, while the remaining background modes are represented by the static expansion (52). When the static expansion is used to eliminate the series representation of the background modes, the quasi-static approximation takes the form

$$(\mathbf{K} - \omega^2\mathbf{M})^{-1} \simeq \frac{\mathbf{u}_1\mathbf{u}_1^{\mathrm{T}}}{\omega_1^2 - \omega^2} + \left(\mathbf{K}^{-1} - \frac{\mathbf{u}_1\mathbf{u}_1^{\mathrm{T}}}{\omega_1^2}\right) \tag{53}$$

The effect of the correction term in Eq. (50) is expressed by the parameter

$$\kappa_1 = \mathbf{w}^{\mathrm{T}}\left(\mathbf{K}^{-1} - \frac{\mathbf{u}_1\mathbf{u}_1^{\mathrm{T}}}{\omega_1^2}\right)\mathbf{w} = \mathbf{w}^{\mathrm{T}}\mathbf{K}^{-1}\mathbf{w} - (v_1/\omega_1)^2 \tag{54}$$

This parameter has a direct physical interpretation, The first term is the displacement between the degrees of freedom of the sensor for a unit force exerted by the actuator, and the second term subtracts the part associated with the first mode. Thus, the parameter κ_1 is an expression of the excess flexibility provided by the background modes. In the computations relating to specific filters it is convenient to use the normalized form

$$\kappa = \kappa_1(\omega_1/v_1)^2 = (v_1/\omega_1)^2\mathbf{w}^{\mathrm{T}}\mathbf{K}^{-1}\mathbf{w} - 1 \tag{55}$$

This parameter is an expression of the relative excess flexibility of the background modes corresponding to an original unit flexibility. It plays a central role in describing the effect of the background modes as demonstrated in the following sections.

The full relation (50) can now be expressed as

$$\mathbf{w}^{\mathrm{T}}\mathbf{q} \simeq -\left[\frac{v_1^2}{G_{qq}(\omega)} + \kappa_1\right] G_{q\eta}(\omega)\eta \tag{56}$$

The final form is obtained by expressing the first term as the modal amplitude by using the homogeneous modal equation (47),

$$\mathbf{w}^{\mathrm{T}}\mathbf{q} \simeq v_1 x_1 - \kappa_1 G_{q\eta}(\omega)\eta \tag{57}$$

When this result is introduced into the control equation (45), the combined set of the non-homogeneous modal equation and the approximate control equation takes the form

$$G_{qq}(\omega)x_1 + v_1 G_{q\eta}(\omega)\eta = F_1$$

$$v_1 G_{\eta q}(\omega)x_1 + [G_{\eta\eta}(\omega) - \kappa_1 G_{\eta q}(\omega)G_{q\eta}(\omega)]\eta = 0 \tag{58}$$

with modal load $F_1 = \mathbf{u}_1^{\mathrm{T}}\mathbf{F}$.

The present equation (58) are in terms of modal components, and therefore are not dimensionally consistent with Eq. (1) for the single-degree-of-freedom system. In the present case it is convenient to use the normalized modal displacement by

$$x = v_1 x_1 = \mathbf{w}^{\mathrm{T}}(\mathbf{u}_1 x_1) \tag{59}$$

This variable has the dimension of displacement, and furthermore takes unit value for unit displacement of the sensor. The corresponding normalized modal force is defined by

$$F = v_1 F_1 = (v_1\mathbf{u}_1)^{\mathrm{T}}\mathbf{F} \tag{60}$$

This load parameter has the dimension [force/mass] = [acceleration]. The modal equation (58) can now be written in the normalized form

$$G_{qq}(\omega)x + v_1^2 G_{q\eta}(\omega)\eta = v_1 F_1$$

$$G_{\eta q}(\omega)x + [G_{\eta\eta}(\omega) - \kappa_1 G_{\eta q}(\omega)G_{q\eta}(\omega)]\eta = 0 \tag{61}$$

The control variable η has the dimension of displacement, when the frequency functions $G_{qq}(\omega)$, $G_{\eta\eta}(\omega)$, $G_{\eta q}(\omega)$ and $v_1^2 G_{q\eta}(\omega)$ have the same dimension, here taken as frequency squared.

The system of equations for modal damping is analogous to the single-degree-of-freedom system (1) provided that the product $G_{\eta q}(\omega)G_{q\eta}(\omega)$ is a quadratic function of frequency, as in the case of displacement feedback. The results for optimal parameters of a single-degree-of-freedom system obtained in Section 4.1 can then be translated into optimal control parameters for the multi-degree-of-freedom system. In the case of acceleration feedback the correspondence is not exact, but a simple modification of the terms in the coupling filters permits the determination of near-optimal parameters. Both cases are treated in the following.

5.2. MDOF system with filtered displacement feedback

The MDOF displacement feedback problem is described by the modal and resonant frequency functions

$$G_{qq}(\omega) = \omega_1^2 - \omega^2, \quad G_{\eta\eta}(\omega) = \omega_\eta^2 - \omega^2 + 2\mathrm{i}\zeta_\eta\omega_\eta\omega \tag{62}$$

and the feedback functions

$$G_{\eta q}(\omega) = \omega_1^2, \quad v_1^2 G_{q\eta}(\omega) = \alpha_\eta\omega^2 + \gamma_\eta 2\mathrm{i}\zeta_\eta\omega_\eta\omega \tag{63}$$

It is to be noted that the function $G_{\eta q}(\omega)$ is here expressed in terms of the original undamped frequency ω_1, while in the SDOF formulation the controller frequency ω_c was used. The reason for the present choice is that it leads to the non-dimensional parameter κ defined in terms of the known structural frequency ω_1, while in the SDOF format the controller frequency ω_c was chosen in order to create greater uniformity between the two types of control.

The task is to express the parameters ω_η, ζ_η, α_η and γ_η in terms of the similar parameters for the single-degree-of-freedom system, and then to use the optimal expressions derived in Section 4.1. This is most easily accomplished by considering the response relation derived from (60),

$$x = \frac{G_{\eta\eta}(\omega) - \kappa_1 G_{\eta q}(\omega) G_{q\eta}(\omega)}{G_{qq}[G_{\eta\eta}(\omega) - \kappa_1 G_{\eta q}(\omega) G_{q\eta}(\omega)] - v_1^2 G_{xy} G_{yx}} v_1 F_1 \tag{64}$$

This formula is similar to Eq. (5) for the SDOF system. In order to have a full analogy the terms in the square brackets should form a function proportional to the frequency function $G_{yy}(\omega)$. Insertion of the relevant frequency functions from Eqs. (62) and (63) gives

$$G_{\eta\eta}(\omega) - \kappa_1 G_{\eta q}(\omega) G_{q\eta}(\omega) = (1 + \alpha_\eta \kappa)[\omega_c^2 - \omega^2 + 2\mathrm{i}\zeta_c \omega_c \omega] \tag{65}$$

where the parameters in the square brackets are given by

$$\omega_c^2 = \frac{1}{1 + \alpha_\eta \kappa} \omega_\eta^2 \tag{66}$$

and

$$\zeta_c \omega_c = \frac{1 - \gamma_\eta \kappa}{1 + \alpha_\eta \kappa} \zeta_\eta \omega_\eta \tag{67}$$

The numerical factor $(1 + \alpha_\eta \kappa)$ is extracted from the last term in the denominator of Eq. (64), and the remainder is recast into the form of the corresponding single-degree-of-freedom expression

$$v_1^2 G_{\eta q}(\omega) G_{q\eta}(\omega) = (1 + \alpha_\eta \kappa) \omega_c^2 [\alpha \omega^2 + \gamma 2\mathrm{i}\zeta_c \omega_1 \omega] \tag{68}$$

When account is taken of the frequency variables appearing in the single-degree-of-freedom format the parameters in the square brackets are found to be

$$\alpha = \frac{\alpha_\eta}{1 + \alpha_\eta \kappa} \frac{\omega_1^2}{\omega_c^2}, \quad \gamma = \frac{\gamma_\eta}{1 + \alpha_\eta \kappa} \frac{\omega_1^2}{\omega_c^2} \frac{\zeta_\eta \omega_\eta}{\zeta_c \omega_1} \tag{69}$$

For optimal parameters the frequency ratio $\omega_1/\omega_c = (1 + \gamma)$ follows from Eq. (23). When the last factor in Eq. (69) is expressed by use of Eq. (67), the relations take the reduced form

$$\alpha = (1 + \gamma)^2 \frac{\alpha_\eta}{1 + \alpha_\eta \kappa}, \quad \gamma = (1 + \gamma) \frac{\gamma_\eta}{1 - \gamma_\eta \kappa} \tag{70}$$

The occurrence of the γ-factor in the power two in the first relation and in the power one in the second relation is due to the difference in frequency normalization between the SDOF and MDOF case. The parameter α is given in terms of γ by Eq. (25), and the two relations are easily inverted to give the MDOF parameters in terms of the gain parameter γ of the equivalent SDOF system,

$$\alpha_\eta = \frac{\gamma(1 - \gamma)}{(1 + \gamma)^2 - \kappa\gamma(1 - \gamma)}, \tag{71a}$$

$$\gamma_\eta = \frac{\gamma}{1 + \gamma + \kappa\gamma} \tag{71b}$$

It follows from relation (71b) that the MDOF gain parameter γ_η is bounded by the upper limit $(1 + \kappa)^{-1}$ corresponding to infinite value of the equivalent SDOF gain γ. Thus, a high value of the background mode parameter κ imposes a stricter limit of the gain γ_η that can be applied to the structure.

5.3. Example: cantilever beam with piezoelectric sensor and actuator

In this example the resonant control with displacement feedback is implemented for a cantilever beam as shown in Fig. 7. Two rectangular piezoelectric strips are placed symmetrically on the top and bottom side of the beam, where they act as a collocated sensor/actuator pair. This type of setup is often used to illustrate the performance of active control strategies on flexible structures, see e.g. Ref. [12]. The actuator strip produces a

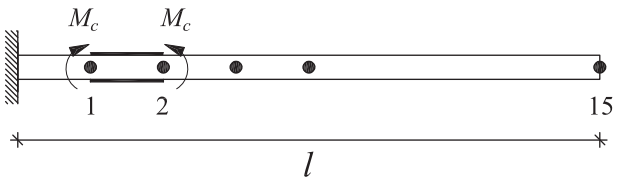

Fig. 7. Cantilever beam with piezoelectric strips as sensor and actuator.

Table 1
Mode 1 damping ratios for cantilever beam ($\kappa = 4.042$).

ζ_1^{des}	ζ_c	γ	ω_c/ω_1	γ_η	α_η	ω_η/ω_1	ζ_η	$\zeta_1^{\mp}$	$\zeta_1^{\mp}\|_{\kappa=0}$
0.03	0.06	0.0072	0.9928	0.0070	0.0073	1.0073	0.0626	0.0299	0.0346
								0.0299	0.0226
0.06	0.12	0.0292	0.9716	0.0255	0.0300	1.0289	0.1417	0.0591	0.0648
								0.0589	0.0341
0.09	0.18	0.0669	0.9373	0.0500	0.0705	1.0624	0.2557	0.0868	0.0749
								0.0866	0.0404
0.12	0.24	0.1218	0.8914	0.0755	0.1295	1.1003	0.4263	0.1124	0.0578
								0.1121	0.0446

pair of control moments proportional to the applied voltage: $M_c = K_p V_{\text{app}}$, where K_p depends on the size and material properties of the piezoelectric strip [13]. On the other hand, the voltage measured by the sensor is proportional to the difference in bending rotation at the two ends of the strip: $\Delta\theta = (C_f/K_p)V_{\text{sen}}$, where C_f is the capacitance of the charge amplifier.

The cantilever beam is made of steel with elastic modulus $E = 2.1 \times 10^{11}\,\text{N/m}^2$ and mass density $\rho = 7850\,\text{kg/m}^3$. The length is $l = 0.75\,\text{m}$, width is $b = 0.05\,\text{m}$ and thickness is $t = 0.005\,\text{m}$. The beam is discretized into 15 identical beam elements with two nodal degrees of freedom (transverse displacement u_i and rotation θ_i). The piezoelectric strips are located between nodes 1 and 2, as indicated in Fig. 7. This means that the length of each strip is 0.05 m and that they are attached 0.05 m from the support. Hereby, the connectivity vector is

$$\mathbf{w}^{\text{T}} = [0, -1, 0, 1, 0 \ldots 0]$$

and the correction factor in Eq. (55) is $\kappa = 4.042$, which indicates significant influence from higher modes. The collocated format of the control implies that $\Delta\theta = \mathbf{w}^{\text{T}}\mathbf{q}$ and the transfer relation between applied and sensor voltage then appears as

$$V_{\text{app}} = -\frac{C_f}{K_p^2}\frac{G_{q\eta}G_{\eta q}}{G_{\eta\eta}}V_{\text{sen}}$$

In practice the design of the control system relies on a desired damping ratio for the critical mode, which in this case is mode 1. Since the present design procedure leads to equal split of the filter damping ζ_c into the two vibration modes, it should be chosen as twice the desired modal damping: $\zeta_c = 2\zeta_1^{\text{des}}$. By inversion of Eq. (26) an expression for the control gain is found as

$$\gamma = -1 + 2\zeta_c^2 + \sqrt{1 + (2\zeta_c^2)^2} \simeq 2\zeta_c^2(1 + \zeta_c^2) \tag{72}$$

where the last relation follows from the two term expansion of the square root. Table 1 gives the design results for a desired damping ratio $\zeta_1^{\text{des}} = 0.03$, 0.06, 0.09 and 0.12, respectively. The design procedure follows the order of the columns in the table. Initially the desired damping ratio ζ_1^{des} for mode 1 is chosen and the filter damping is $\zeta_c = 2\zeta_1^{\text{des}}$. Then the gain parameter γ of the SDOF system is found by Eq. (72) and the filter

frequency ω_c for the SDOF system is determined by Eq. (23). Finally, the control gains α_η and γ_η are computed by Eq. (71b), and the filter parameters ω_η and ζ_η of the actual filter in the MDOF case are determined by Eqs. (66) and (67), respectively. The second last column of the table gives the two damping ratios for the two branches associated with mode 1, found by an eigenvalue analysis of the full system. It is seen from the table that there is almost perfect equal split of the desired damping into the two modes, i.e. $\zeta_1^- \simeq \zeta_1^+ \simeq \zeta_1^{\mathrm{des}}$. The last column contains the similar damping ratios obtained by use of a control system designed using $\kappa = 0$, i.e. neglecting the influence of the background modes. In this case equal split of modal damping is not attained, and the damping ratio is considerably smaller than that obtained when accounting for the background modes.

Fig. 8 shows the two root loci associated with the split mode 1, with γ as control gain. The markers represent the complex natural frequencies for the four levels of control indicated in Table 1. The solid curves and dots represent frequency loci for a control design with κ included, whereas the dashed curves and crosses represent the case with $\kappa = 0$. It is seen that the frequency loci for both cases emanate from the undamped mode 1 frequency under 45°, as discussed earlier for the SDOF system in connection with Fig. 3. The solid curve follows the 45° trajectory fairly well and provide almost perfect equal split of modal damping for all four dots, as illustrated for the last set of roots with $\gamma = 0.1218$ by the dotted line. In contrast, the dashed curves for $\kappa = 0$ loose the equal damping property quite early and provide substantially less damping. Furthermore, for $\kappa = 0$ the system becomes unstable around $\gamma = 0.21$, where the left (dashed) branch in Fig. 8 moves into the negative imaginary half-plane.

The frequency response of the beam is computed by applying a transverse harmonic force of unit magnitude at the beam tip:

$$\mathbf{F}^{\mathrm{T}} = [0, 0, \ldots, 1, 0] \exp(\mathrm{i}\omega t)$$

The response is obtained by solving for $\mathbf{q}$ in Eqs. (44) and (45). Fig. 9 shows the dynamic amplification of the transverse tip displacement and magnitude of the moment applied by the piezoelectric actuator. The four

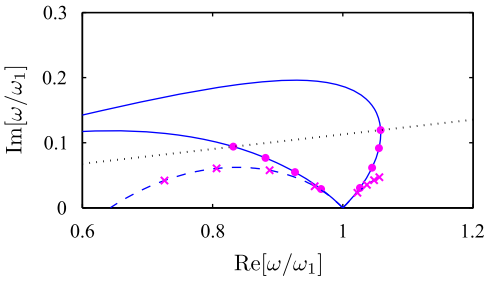

Fig. 8. Root locus diagram. Calibration with (——) and without (– – –) background correction. Markers represent the four cases in Table 1.

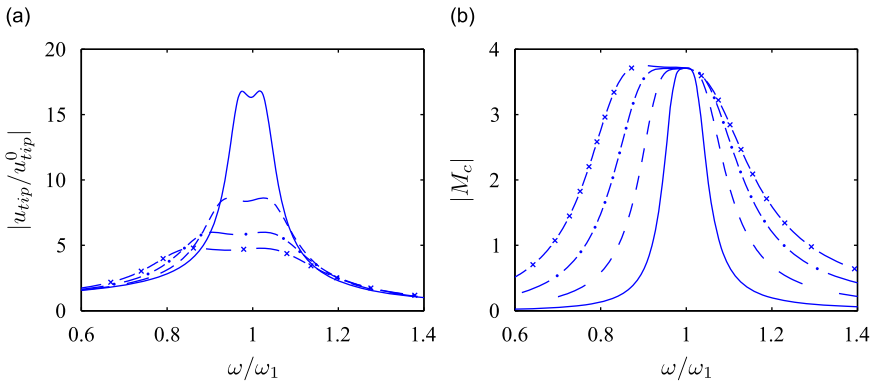

Fig. 9. (a) Dynamic amplification at beam tip. (b) Magnitude of control moment. $\gamma = 0.0072$ (——), 0.0292 (– – –), 0.0669 (– · –) and 0.1218 (– × –).

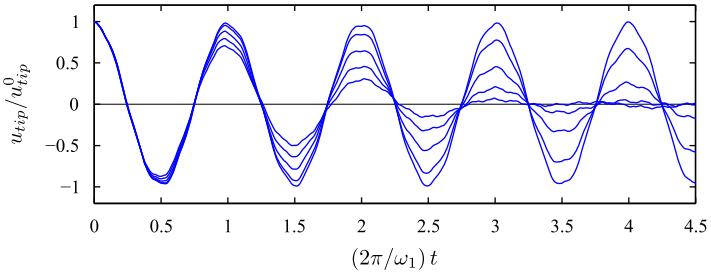

Fig. 10. Free vibration of cantilever beam for $\gamma = 0$ and $\gamma = 0.0072$, 0.0292, 0.0669, 0.1218 from Table 1.

curves represent the four cases in Table 1. Good qualitative agreement is observed when compared to the frequency response curves in Fig. 5 for a single-degree-of-freedom structure.

Finally, the free vibration decay of the cantilever beam is illustrated by time simulations in Fig. 10. The initial displacement is the static deflection when applying the unit tip load. The figure shows the undamped response of the beam and the damped response for the four levels of control in Table 1. It is seen that larger value of γ leads to faster attenuation of the response, while introducing an increasing amount of high frequency components due to control spill-over to the higher modes.

5.4. MDOF system with filtered acceleration feedback

In the case of acceleration feedback the structural response and the controller frequency functions are again given by Eq. (62). However, the feedback functions are now given in a format similar to Eqs. (32) and (33) as

$$G_{\eta q}(\omega) = \omega^2, \quad v_1^2 G_{q\eta}(\omega) = \alpha_\eta \omega_1^2 + \gamma_\eta 2\mathrm{i}\zeta_\eta \omega_\eta \omega \tag{73}$$

Also in this case the identification of the correspondence between the actual MDOF system parameters and ω_η, ζ_η, α_η, γ_η and the equivalent SDOF parameters will be established by use of the displacement frequency response relation (64). First the terms in the square brackets are written in the normalized form

$$G_{\eta\eta}(\omega) - \kappa_1 G_{\eta q}(\omega) G_{q\eta}(\omega) = \omega_\eta^2 - (1 + \alpha_\eta \kappa)\omega^2 + 2\mathrm{i}\zeta_\eta \omega_\eta \omega \left[1 - \gamma_\eta \kappa \frac{\omega^2}{\omega_1^2}\right] \tag{74}$$

The term containing the factor γ_η is a correction term, which is primarily of importance around resonance. When introducing the approximation $\omega^2/\omega_1^2 \sim 1$ in this term, the expression in Eq. (74) takes the same form as Eq. (65) for the case of displacement feedback. Thus, the equivalence between coefficients leads to the frequency relation (66) and damping relation (67) already established for the case of displacement feedback.

The second set of relations is established from the last term of the response function denominator, i.e. by the equation

$$v_1^2 G_{\eta q}(\omega) G_{q\eta}(\omega) = (1 + \alpha_\eta \kappa)\omega^2 [\alpha \omega_c^2 + \gamma 2\mathrm{i}\zeta_c \omega_c \omega] \tag{75}$$

The gain factors α and γ of this expression are identified by comparison with the product formed from the MDOF frequency functions in (73):

$$\alpha = \frac{\alpha_\eta}{1 + \alpha_\eta \kappa} \frac{\omega_1^2}{\omega_c^2}, \quad \gamma = \frac{\gamma_\eta}{1 + \alpha_\eta \kappa} \frac{\zeta_\eta \omega_\eta}{\zeta_c \omega_c} \tag{76}$$

It is seen that while the relation for the α-gain factor is identical to that of displacement control, the γ-gain factor now depends directly on the ratio of the combined damping frequency product. When the last factor in these two relations are expressed by the optimal frequency ratio and the optimal damping ratio via Eq. (67), the result is

$$\alpha = (1 + \gamma)^2 \frac{\alpha_\eta}{1 + \alpha_\eta \kappa}, \quad \gamma = \frac{\gamma_\eta}{1 - \gamma_\eta \kappa} \tag{77}$$

In the present case it follows from Eq. (38) that $\alpha = \gamma$, and the inverse relations for the gain factors are then found as

$$\alpha_\eta = \frac{\gamma}{(1+\gamma)^2 - \kappa\gamma}, \tag{78a}$$

$$\gamma_\eta = \frac{\gamma}{1+\kappa\gamma} \tag{78b}$$

These relations together with Eqs. (66) and (67) enable determination of the damping parameters in terms of the single gain parameter γ for an MDOF structure with an actuator controlled by filtered acceleration feedback.

5.5. Example: cable with collocated accelerometer and actuator

Fig. 11 shows a taut stay cable of length l with a transverse actuator acting on the cable at the distance $l_d = 0.02l$ from the bottom support. It is known that an optimally tuned linear viscous damper leads to a modal damping ratio of $\zeta_1^{\max} = \frac{1}{2} l_d/l = 0.01$ [23]. This serves as a reference value for the efficiency of the present optimally calibrated resonance damper.

The cable is discretized into 50 elements with the actuator attached to node 1. Linear interpolation with lumped mass is used leading to the mass and stiffness matrices

$$\mathbf{M} = m_{\text{cab}} \begin{bmatrix} 1 & & & \\ & 1 & & \\ & & \ddots & \\ & & & 1 \end{bmatrix}, \quad \mathbf{K} = k_{\text{cab}} \begin{bmatrix} 2 & -1 & & \\ -1 & 2 & & \\ & & \ddots & -1 \\ & & -1 & 2 \end{bmatrix}$$

The concentrated nodal masses are taken as $m_{\text{cab}} = 1$ and the element stiffness k_{cab} is chosen so that the natural frequency of the first mode is $\omega_1 = 2\pi = 6.283$, corresponding to a vibration period of 1.00 for mode 1. Acceleration feedback is assumed via an ideal accelerometer attached to the cable at the location of the actuator. The connectivity vector of the collocated system is

$$\mathbf{w}^{\mathrm{T}} = [1, 0, 0, \ldots, 0]$$

This gives a correction factor for background modes of $\kappa = 23.52$, indicating a significantly larger influence of higher modes for the present cable example than for the cantilever beam used in the previous example for displacement feedback control.

The design procedure for the acceleration feedback control is similar to that for displacement feedback. The desired damping ratio is split equally between the two modes generated by the resonant actuator. Thus, the SDOF damping ratio is $\zeta_c = 2\zeta_1^{\text{des}}$, and upon inversion of Eq. (39) the parameter γ is determined by

$$\gamma = \frac{2\zeta_c^2}{1 - 2\zeta_c^2} \tag{79}$$

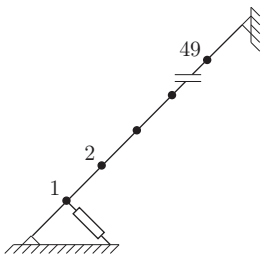

Fig. 11. Taut stay cable with damper attached at node 1.

The results of the design procedure are summarized in Table 2 for desired damping ratios $\zeta_1^{\text{des}} = 0.01$, 0.02, 0.04 and 0.06. The split of the damping ratio on the two resulting vibration modes is nearly equal, although not quite as good as for the cantilever beam with displacement feedback. This is due to the greater influence of the background modes, that is accounted for via a quasi-static approximation. Compared to the optimal viscous damping with $\zeta^{\max} = 0.01$ the present resonant control performs very well, enabling a modal damping ratios of around $\zeta^{\pm} \simeq 0.06$, corresponding to six times that of passive viscous damping. The larger influence of the background modes in the present case also leads to further shortcomings of a design without including their effect, i.e. a design based on $\kappa = 0$.

Fig. 12 shows the root locus diagram of the cable with an optimally controlled actuator. It is seen that the solid curves follow the 45° trajectory almost up to the stability limit, determined as the value of γ for which the expression (78a) for α_η becomes unbounded. With the present value of $\kappa = 23.52$ this corresponds to a stability limit of $\gamma = 0.046$. The four levels of control listed in Table 2 are indicated by dots. The dashed line connects the origin and the point on the right branch for $\gamma = 0.0297$. The deviation from the equal split condition is illustrated in terms of the corresponding dot on the left branch. Although the deviation is visible it is perfectly acceptable for design purposes. The similar results corresponding to a design without accounting for the effect of the undamped modes, i.e. with $\kappa = 0$, are shown by the dashed curves and cross markers. It is clearly illustrated that a design without account of undamped modes is insufficient and leads to low and unequal modal damping not exceeding that of an optimal passive viscous damper.

A frequency response analysis is conducted for a uniformly distributed harmonic load with unit nodal intensity

$$\mathbf{F}^{\mathrm{T}} = [1, 1, \ldots, 1] \exp(\mathrm{i}\omega t)$$

The dynamic amplification of the cable midspan response is shown in Fig. 13a and the magnitude of the frequency response of the actuator force is shown in Fig. 13b. The flat plateau is again obtained in the mid span response and the control force has a positive inclination similar to that for the SDOF case in Fig. 6. It

Table 2
Mode 1 damping ratios for cable ($\kappa = 23.52$).

ζ_1^{des}	ζ_c	γ	ω_c/ω_1	γ_η	α_η	ω_η/ω_1	ζ_η	$\zeta_1^{\mp}$	$\zeta_1^{\mp}\vert_{\kappa=0}$
0.01	0.02	0.0008	0.9992	0.0008	0.0008	1.0087	0.0206	0.0101 0.0098	0.0136 0.0059
0.02	0.04	0.0032	0.9968	0.0030	0.0034	1.0364	0.0447	0.0205 0.0194	0.0285 0.0072
0.04	0.08	0.0130	0.9872	0.0099	0.0180	1.1776	0.1245	0.0418 0.0376	0.0470 0.0067
0.06	0.12	0.0297	0.9712	0.0175	0.0818	1.6607	0.3483	0.0647 0.0549	0.0502 0.0055

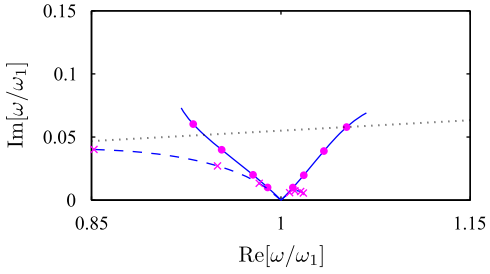

Fig. 12. Root locus diagram. Calibration with (——) and without (– – –) background correction. Markers represent the four cases in Table 2.

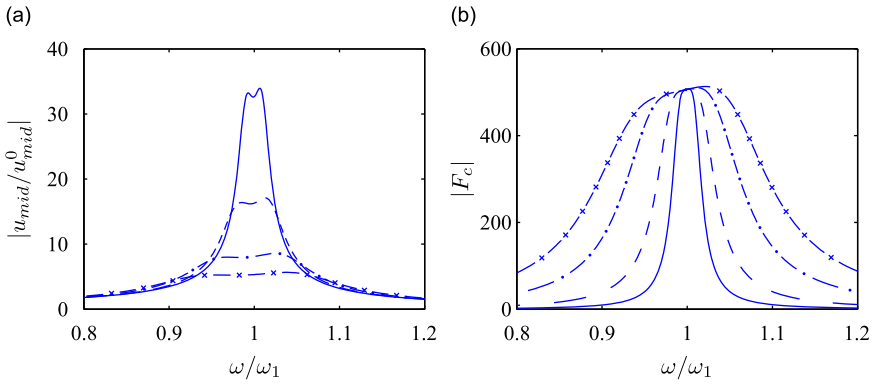

Fig. 13. (a) Dynamic amplification at cable mid. (b) Magnitude of control force. $\gamma = 0.0008$ (——), 0.0032 (– – –), 0.0130 (– · –) and 0.0297 (– × –).

should be noted that the scales on the axes have been changed by a factor of 2 due to the lower level of damping in the present example.

6. Conclusions

The general principle of resonant control consists in the introduction of a resonant circuit or device, connected to the structure via feedback of a sensor and an actuator. The present paper describes a design philosophy and its practical implementation. The coupling of the control resonator to the structure leads to a split of the original resonant mode into two modes. The first design condition introduced here is that these two modes should have identical modal damping ratio. This is attained by a root locus analysis, that gives a particular mathematical format and determines the resonator's natural frequency in terms of a feedback parameter. The next concern regards the relative frequencies of the two resonant peaks. If the resonant frequencies are close, the two modes interfere, eventually forming a single broadened peak if too close. Thus, optimal separation of the two resonance peaks forms the second design consideration. This consideration is implemented via a requirement of equal amplification at two special points, at which the combined amplification is independent of damping. Finally, the damping coefficient of the resonant controller is selected to provide a flat plateau of the frequency response curve. The procedure is described in detail for filtered displacement feedback and for filtered acceleration feedback in Section 4. There are only modest differences between the formulae for the optimal parameters in the two cases, and both forms lead to similar response characteristics.

The extension to the case of multi-degree-of-freedom systems is also presented. The important point is that in these systems the actuator will typically activate response from other modes than the one selected for control. These other modes—the background modes—contribute to the response picked up by the sensor. It is important to counteract this effect in the calibration of the resonant controller. A simple explicit procedure, in which the background modes are included via a quasi-static approximation is described. This procedure leads to an explicit modification of the formulae for the optimal controller parameters, and thus the complete calibration retains its non-iterative form. The importance of including the effect of background modes is illustrated by examples, where the method which includes the effect of background modes retains near-ideal properties of the resulting response. In contrast, straightforward application of the design formulae for the single-degree-of-freedom system to flexible structures leads to severe deterioration of the efficiency of the resonant controller.

Appendix A. Root locus analysis

This appendix presents the topology and a parameter representation of the root locus diagram under the condition of equal modal damping. The inverse root property of the characteristic equation (9) leads to a fairly

simple complete solution for all parameter values. It follows from the equivalent form (8) that the characteristic equation is a quadratic equation in the variable

$$\mathrm{i}\xi = \frac{1}{2}\left(\frac{\omega}{\omega_0} - \frac{\omega_0}{\omega}\right) \tag{A.1}$$

with solution

$$\xi/c = \beta \mp \sqrt{\beta^2 - 1} \tag{A.2}$$

The frequency ratio ω/ω_0 then follows from the definition of ξ in Eq. (A.1) as

$$\omega/\omega_0 = \mathrm{i}\xi \pm \sqrt{1 - \xi^2} \tag{A.3}$$

The four roots ω_j are generated by the four sign combinations in Eqs. (A.2) and (A.3).

The parameter β appears as a factor to the imaginary coefficients in the characteristic equation and is associated with the damping of the coupled system. It is therefore natural to start the root locus analysis with considering the roots for $\beta = 0$. For this parameter value (A.2) gives $\xi = \mp \mathrm{i}c$. Substitution of these values into Eq. (A.3) then demonstrates that there are two different cases, depending on whether the parameter c is smaller or greater than unity. It appears that in the cases of interest in the present context $c \leqslant 1$, and this will be assumed in the following. Under this condition the roots ω_1 and ω_2 are located on the positive real axis and found from Eq. (A.3) with $\xi = \mp \mathrm{i}c$ as

$$\omega_{1,2}/\omega_0|_{\beta=0} = \mp c + \sqrt{1 + c^2} \tag{A.4}$$

Thus, the condition $c \leqslant 1$ corresponds to the condition of real-valued natural frequencies for $\beta = 0$. In this case the parameter c defines the difference between the frequencies ω_1 and ω_2 for $\beta = 0$,

$$\omega_2 - \omega_1 = 2c\omega_0 \tag{A.5}$$

This relation is illustrated in Fig. 2, where the difference between the roots on the real axis is $2c = 0.8$. The markers correspond to $\beta = 0, 0.05, 0.10, 0.15, \ldots$.

When the parameter β is increased from zero the roots ω_1, ω_2 and ω_3, ω_4 generate curves that meet at two bifurcation points for $\beta = 1$, corresponding to $\xi = c$ and

$$\omega_b/\omega_0 = \mathrm{i}c \pm \sqrt{1 - c^2} \tag{A.6}$$

When β increases beyond the value $\beta = 1$ the roots leave the bifurcation points following the circle $|\omega| = \omega_0$ as illustrated in Fig. 2. The two upper branches meet at a new bifurcation point $\omega = \mathrm{i}\omega_0$ at the imaginary axis. It follows directly from the root locus equation (9) that this bifurcation point is reached at

$$\beta = \tfrac{1}{2}(c + c^{-1}) \tag{A.7}$$

It is noted that the first pair of bifurcation points are located on the circle $|\omega| = \omega_0$, irrespective of the value of the parameter c.

Appendix B. Optimal amplification characteristics

In this appendix two optimality conditions are obtained from the frequency curve of the amplification of the structural response. The first condition follows from the observation that the frequency curve of the amplification has two fix points at ω_A and ω_B, where the amplification is independent of the damping parameter ζ_c of the controller as illustrated in Fig. 4. A relation between the remaining parameters is obtained by imposing the condition of equal amplification at ω_A and ω_B. This generalizes the procedure introduced in Ref. [1] for the special case of the tuned mass absorber. The special fix point property follows from the observation that the frequency response function is of the form

$$\frac{xk}{F} = \frac{A + 2\mathrm{i}\zeta_c B}{C + 2\mathrm{i}\zeta_c D} \tag{B.1}$$

where A, B, C, D depend on the frequency, but are independent of the parameter ζ_c. The format (B.1) implies that in order for the response magnitude to be independent of the parameter ζ_c, the coefficient functions must satisfy the equation

$$AB = \pm BD \tag{B.2}$$

It turns out that only the condition with the minus sign leads to an equation for the fix point frequencies ω_A and ω_B. In the present formulation this equation determines the parameter α in terms of γ.

The second condition follows from the requirement that the amplification at the reference frequency ω_0, located between the fix point frequencies ω_A and ω_B is equal to the amplification at these frequencies as illustrated in Fig. 4,

$$\left|\frac{xk}{F}\right|_{\omega_0} = \left|\frac{xk}{F}\right|_{A,B} \tag{B.3}$$

This generalizes the procedure introduced for determining the optimal damping of the tuned mass absorber in Ref. [17] and provides an equation of the parameter ζ_c.

B.1. Filtered displacement feedback

In the case of displacement feedback the displacement frequency response function of x follows from Eqs. (4) and (20) as

$$\frac{xk}{F} = \frac{\omega_0^2[\omega_0^2 - (1+\gamma)\omega^2 + 2\mathrm{i}\sqrt{1+\gamma}\zeta_c\omega_0\omega]}{\omega^4 - \left(2 + \dfrac{\alpha+\gamma^2}{1+\gamma}\right)\omega_0^2\omega^2 + \omega_0^4 + \dfrac{2\mathrm{i}\zeta_c}{\sqrt{1+\gamma}}\omega_0\omega(\omega_0^2 - \omega^2)} \tag{B.4}$$

where $k = \omega_s^2 m$ is the structural stiffness. The first step is to form Eq. (B.2) with the minus sign. In the present case the response function (B.4) leads to the equation

$$2(1+\gamma)\omega^4 - (4 + \alpha + 3\gamma + \gamma^2)\omega_0^2\omega^2 + (2+\gamma)\omega_0^2 = 0 \tag{B.5}$$

This quadratic equation for ω^2 implies that the sum of the roots is given by the coefficients to the middle term divided by the coefficient to the first term

$$\omega_A^2 + \omega_B^2 = \frac{4 + \alpha + 3\gamma + \gamma^2}{2(1+\gamma)}\omega_0^2 \tag{B.6}$$

At the frequencies ω_A and ω_B the amplification is independent of ζ_c, and it can therefore be evaluated from the limit $\zeta_c \to \infty$ as the ratio of the coefficients B and D. When accounting for a reversal of phase angle this relation is

$$\frac{\omega_0^2}{\omega_0^2 - \omega_A^2} = \frac{\omega_0^2}{\omega_B^2 - \omega_0^2} \tag{B.7}$$

from which

$$\omega_A^2 + \omega_B^2 = 2\omega_0^2 \tag{B.8}$$

The fix point frequencies are determined by equating the right sides of the two Eqs. (B.6) and (B.8), leading to the relation

$$\alpha = \gamma(1-\gamma) \tag{B.9}$$

This relation enables elimination of the gain parameter α.

The fix point frequencies are needed for evaluation of the amplification. They follow from Eq. (B.5) as

$$\frac{\omega_{A,B}^2}{\omega_0^2} = 1 \mp \sqrt{\frac{\gamma}{2(1+\gamma)}} \tag{B.10}$$

At the frequencies ω_A and ω_B the amplification is independent of the parameter ζ_c, and it can therefore be determined directly from the ratio of the imaginary parts of the response function,

$$\left|\frac{xk}{F}\right|_{A,B} = (1+\gamma)\sqrt{\frac{2(1+\gamma)}{\gamma}} \tag{B.11}$$

At the reference frequency ω_0 the response is found to be

$$\left.\frac{xk}{F}\right|_{\omega_0} = (1+\gamma)\left[1 - 2\mathrm{i}\zeta_c\sqrt{\frac{1+\gamma}{\gamma}}\right] \tag{B.12}$$

The control parameter ζ_c is determined by equating the amplification factor at the three frequencies, whereby

$$\zeta_c^2 = \frac{\gamma}{4}\frac{2+\gamma}{1+\gamma} \tag{B.13}$$

This completes the determination of optimal parameters α and ζ_c in terms of the gain parameter γ for the case of filtered displacement feedback.

When this design procedure for filtered displacement feedback is compared to the generic root locus format in Section 3 it is found that it corresponds to

$$\beta = \frac{1}{2}\sqrt{\frac{2+\gamma}{1+\gamma}} \simeq \frac{\sqrt{2}}{2}\left(1 - \frac{1}{4}\gamma + \cdots\right), \quad c = \frac{1}{2}\sqrt{\frac{\gamma}{1+\gamma}} \tag{B.14}$$

Thus, for typical values of γ in the order of 0.01–0.05 it is seen that $\beta \simeq \frac{1}{2}\sqrt{2}$, as discussed at the end of Section 3. Furthermore, it is seen that $c < \frac{1}{2}$, and thus the complex roots always correspond to inverse points located on the small circle in Fig. 2.

B.2. Filtered acceleration feedback

In the case of acceleration feedback the structural frequency response function follows from Eqs. (4) and (34) as

$$\frac{xk}{F} = \frac{\omega_0^2[\omega_0^2 - (1+\gamma)\omega^2 + 2\mathrm{i}\sqrt{1+\gamma}\zeta_c\omega_0\omega]}{\omega^4 - \left(2 + \dfrac{\alpha+\gamma^2}{1+\gamma}\right)\omega_0^2\omega^2 + \omega_0^4 + 2\mathrm{i}\sqrt{1+\gamma}\zeta_c\omega_0\omega(\omega_0^2 - \omega^2)} \tag{B.15}$$

The procedure for determination of the parameters α and ζ_c closely follows that of the corresponding displacement feedback problem. In the present case condition (B.2) takes the form

$$(2+\gamma)\omega^4 - \left(4 + \gamma + \frac{\alpha+\gamma^2}{1+\gamma}\right)\omega_0^2\omega^2 + 2\omega_0^4 = 0 \tag{B.16}$$

This quadratic equation for ω^2 implies that the sum of the roots is given by the coefficients to the middle term divided by the coefficient of the first term,

$$\omega_A^2 + \omega_B^2 = \frac{4 + \gamma + \dfrac{\alpha+\gamma^2}{1+\gamma}}{2+\gamma}\omega_0^2 \tag{B.17}$$

The amplification at ω_A and ω_B is assumed to be independent of the parameter ζ_c and can therefore be evaluated from ratio of the coefficients B and D. As in the previous case this leads to Eq. (B.8). Equality of the right sides of Eqs. (B.17) and (B.8) then gives

$$\alpha = \gamma \tag{B.18}$$

Thus, in this case equal amplification at the two fix points leads to equality of the two gain factors.

When the amplification factors are taken to be equal in accordance with Eq. (B.18) the expressions simplify and the fix point frequencies follow from Eq. (B.16) as

$$\frac{\omega_{A,B}^2}{\omega_0^2} = 1 \mp \sqrt{\frac{\gamma}{2+\gamma}} \tag{B.19}$$

At the frequencies ω_A and ω_B the amplification is independent of the parameter ζ_c, and the amplification can therefore be determined directly from the coefficient ratio B/D,

$$\left|\frac{xk}{F}\right|_{A,B} = \sqrt{\frac{2+\gamma}{\gamma}} \tag{B.20}$$

At the reference frequency ω_0 the response follows from Eq. (B.15) as

$$\left.\frac{xk}{F}\right|_{\omega_0} = 1 - 2\mathrm{i}\zeta_c\sqrt{\frac{1+\gamma}{\gamma}} \tag{B.21}$$

By setting the corresponding response amplitude equal to Eq. (B.20), an equation is obtained for ζ_c with the solution

$$\zeta_c^2 = \frac{1}{2}\frac{\gamma}{1+\gamma} \tag{B.22}$$

This completes the determination of optimal parameters α and ζ_c in terms of the gain parameter γ for the case of filtered acceleration feedback.

In this case the corresponding generic parameters from the root locus analysis in Section 3 correspond to

$$\beta = \tfrac{1}{2}\sqrt{2}, \quad c = \tfrac{1}{2}\sqrt{\gamma} \tag{B.23}$$

This matches the design parameter combination discussed in Section 3 exactly.

References

[1] J.P. Den Hartog, *Mechanical Vibrations*, fourth ed., McGraw-Hill, New York, 1956.
[2] M.J. Balas, Direct velocity feedback control of large space structures, *Journal of Guidance and Control* 2 (1979) 252–253.
[3] C.J. Goh, T.K. Caughey, On the stability problem caused by finite actuator dynamics in the collocated control of large space structures, *International Journal of Control* 41 (3) (1985) 787–802.
[4] J.L. Fanson, T.K. Caughey, Positive position feedback control for large space structures, *AIAA Journal* 28 (4) (1990) 717–724.
[5] E. Sim, S.W. Lee, Active vibration control of flexible structures with acceleration feedback, *Journal of Guidance, Control, and Dynamics* 16 (1993) 413–415.
[6] J.-N. Juang, M. Phan, Robust controller designs for second-order dynamic systems: a virtual passive approach, *Journal of Guidance, Control, and Dynamics* 15 (5) (1992) 1192–1198.
[7] C.J. Goh, W.Y. Yan, Approximate pole placement for acceleration feedback control of flexible structures, *Journal of Guidance, Control, and Dynamics* 19 (1996) 256–259.
[8] M.P.B. de Noyer, S.V. Hanagud, Single actuator and multi-mode acceleration feedback control, *Journal of Intelligent Material Systems and Structures* 9 (7) (1998) 522–533.
[9] J.-N. Juang, Optimal design of a passive vibration absorber for a truss beam, *Journal of Guidance, Control, and Dynamics* 7 (6) (1984) 733–739.
[10] G. Lee-Glauser, J.-N. Juang, J.L. Sulla, Optimal active vibration absorber: design and experimental results, *Journal of Vibration and Acoustics* 117 (1995) 165–171.
[11] S.-T. Wu, Virtual vibration absorbers with inherent damping, *Journal of Guidance, Control, and Dynamics* 25 (4) (2002) 644–650.
[12] H.R. Pota, S.O. Reza Moheimani, M. Smith, Resonant controllers for smart structures, *Smart Materials and Structures* 11 (2002) 1–8.
[13] A. Preumont, *Vibration Control of Active Structures. An Introduction*, second ed., Kluwer Academic Publishers, Dordrecht, 2002.
[14] G.J. Lee-Glauser, G. Ahmadi, L.G. Horta, Integrated passive/active vibration absorber for multistory buildings, *Journal of Structural Engineering* 123 (1997) 499–504.
[15] J. Ormondroyd, J.P. Den Hartog, The theory of the dynamic vibration absorber, *Transactions of the ASME* 50 (1928) 9–22.
[16] J.E. Brock, A note on the damped vibration absorber, *Journal of Applied Mechanics ASME* 13 (1946) A284.
[17] S. Krenk, Frequency analysis of the tuned mass damper, *Journal of Applied Mechanics ASME* 72 (2005) 936–942.
[18] S. Krenk, A. Brønden, A. Kristensen, Placement and tuning of resonance dampers on footbridges, FOOTBRIDGE 2005, in: 2*nd International Conference*, Venice, Italy, December 6–8, 2005 (CD-Rom).

[19] M.B. Ozer, T.J. Royston, Application of Sherman–Morrison matrix inversion formula to damped vibration absorbers attached to multi-degree of freedom systems, *Journal of Sound and Vibration* 283 (2005) 1235–1249.
[20] M.B. Ozer, T.J. Royston, Extending Den Hartog's vibration absorber technique to multi-degree of freedom systems, *Journal of Vibration and Acoustics* 127 (2005) 341–350.
[21] S. Krenk, J. Høgsberg, Tuned mass absorbers on damped structures under random load, *Probabilistic Engineering Mechanics* 23 (2008) 408–415.
[22] O.E. Hansteen, K. Bell, Accuracy of mode superposition analysis in structural dynamics, *Earthquake Engineering and Structural Dynamics* 7 (1979) 405–411.
[23] S. Krenk, Vibrations of a taut cable with an external damper, *Journal of Applied Mechanics* 67 (2000) 772–776.